Conformational Phase Transitions Associated with Reversal of Hydrogen Bond Direction in 4-Chloro- and 4-Bromobenzyl Alcohols. An X-Ray Study

Masao Hashimoto and Michiko Harada

Department of Chemistry, Faculty of Science, Kobe University, Nadaku, Kobe 657-8501, Japan

Reprint requests to Dr. M. H.; E-mail: mhashi@kobe-u.ac.jp

Notable changes in the molecular conformations of 4-chlorobenzyl alcohol around the $C(H_2)$-C_{ar} and O-$C(H_2)$ bonds were found to take place at the first-order phase transition point ($T_{c1} = 236$ K). Quite similar phenomena were observed at T_{c1} (217 K) of the isomorphic 4-bromo compound. The two kinds of conformational changes are considered to couple and cause the reversal of the direction of the linear O-$H\ldots O$ hydrogen bond as the compound undergoes the first-order transition. The CH_2OH moiety participates in several short intermolecular contacts, and a C-$H\ldots\pi$ interaction exists between the CH_2 and the neighboring phenyl group. These intermolecular factors seem to contribute to the regulation of the molecular conformation in the crystal. The C-O bond length of each compound shortens considerably at $T > T_{c1}$.

Key words: Crystal Structure; Phase Transition; Hydrogen Bond; Molecular Conformation.

1. Introduction

Several types of conformational phase transitions are known [1]. In the crystal of dimethyl 3,6-dichloro-2,5-dihydroxyterephthalate, for example, a functional group attached to the phenyl ring rotates around the C-C_{ar} bond during the phase transition [2]. In a previous paper we reported a similar phenomenon observed for 4-methylbenzyl alcohol (*p*MBA) [3], in which the first-order phase transition at 211 K is accompanied by a remarkable change in the molecular conformations around the $C(H_2)$-C_{ar} bond. In this case, moreover, the conformation around the O-$C(H_2)$ bond also exhibits a drastic jump at the transition point.

The title compounds, 4-chloro- and 4-bromobenzyl alcohols (*p*CBA and *p*BBA, respectively) are known to undergo first- and higher-order phase transitions at T_{c1} and T_{c2}, respectively; (T_{c1}, T_{c2}): (236, 217 K) for *p*CBA; (217, 195 K) for *p*BBA [4, 5]. The crystal structure of *p*CBA at room temperature is known [6], and a preliminary X-ray powder diffraction experiment suggested quite similar crystal structures for the three phases of *p*CBA [7].

In the course of our recent study on the crystal dynamics of these compounds by ^2H NMR we determined their crystal structure at various temperatures in the range $130 < T/K < 300$ by single crystal X-ray diffraction. The crystal dynamics were already discussed in [8], where a part of the crystallographic data was given. In addition to our previous report on these compounds we will present here detailed results of the crystallographic investigation. The three crystalline phases of the compounds will be referred to as low-, intermediate- and room-temperature phase (abbreviated as LTP, ITP, and RTP, respectively).

2. Experimental

The single crystals of *p*CBA were grown from an ethanol-water solution, and those of *p*BBA were selected from the commercial compound (nacalai tesque) without further treatment, and also from sublimed material. Details of the single crystal X-ray experiment are summarized in Table 1. The diffraction data of *p*CBA and *p*BBA were collected at 8 and 13 temperatures, respectively. The lattice parameters were determined at several additional temperatures, too.

The structures of both compounds were solved by direct methods and refined by full-matrix least-squares calculations using the program package SHELXL-97 [9]. Absorption correction was applied by an empirical method (SADABS). All non-hydrogen atoms of

	*p*CBA (LTP)	*p*CBA (RTP)	*p*BBA (LTP)	*p*BBA (RTP)
Formula	— C_7H_7OCl —		— C_7H_7OBr —	
Formula weight	142.58		187.04	
Temperature	133 K	240 K	133 K	220 K
Crystal system	monoclinic	monoclinic	monoclinic	monoclinic
Space group	$P2_1$	$P2_1$	$P2_1$	$P2_1$
a/A	5.876(1)	5.886(2)	6.076(1)	6.047(1)
b/A	4.795(1)	4.900(1)	4.807(1)	4.923(1)
c/A	12.018(3)	12.013(3)	12.147(2)	12.113(2)
β	101.592(4)	102.420(4)	101.312(3)	102.237(3)
V/A^3	331.7(1)	338.4(2)	347.9(1)	352.4(1)
Z	2	2	2	2
D_x/g·cm^{-3}	1.427	1.399	1.786	1.763
μ(Mo K$_\alpha$)/mm^{-1}	0.480	0.470	5.817	5.742
F(000)	148	148	184	184
Crystal dimensions	0.43·0.37·0.16	0.43·0.37·0.16	0.39·0.30·0.10	0.27·0.22·0.15
Radiation	— Graphite monochromated Mo-K$_\alpha$ —			
$R(F_o)$ [$I > 2\sigma(I)$]	0.0400	0.0436	0.0423	0.0484
$R_w(F_o{}^2)$ [for all data]	0.1084	0.1201	0.1020	0.1330
Reflections collected	1749	1780	1629	1726
Independent reflections	1114	1133	1128	1168
R(int)	0.0442	0.0338	0.0335	0.0317
Obs. reflections [$I > 2\sigma(I)$]	1085	1075	1079	1101
No. of parameters	110	110	86	86
θ_{max}/°	27.04	26.89	27.07	27.00
$(\Delta/\sigma)_{max}$	0.001	0.000	0.000	0.000
$(\Delta\rho)_{max}$/e A^{-3}	0.358	0.345	1.226	0.974
$(\Delta\rho)_{min}$/e A^{-3}	–0.329	–0.228	–1.070	–1.198
Diffractometer	— BRUKER SMART 1000 —			
Weighting scheme	$w = 1/[\sigma^2(F_o{}^2) + c_1 P + (c_2 P)^2]$, $P = (F_o{}^2 + 2F_c{}^2)/3$			
c_1; c_2	0.0379; 0.0869	0.0519; 0.0861	0; 0.0631	0; 0.1184
Absorption correction	SADABS		SADABS	

Table 1. Crystal data and details of experiment and refinement for *p*CBA and *p*BBA.
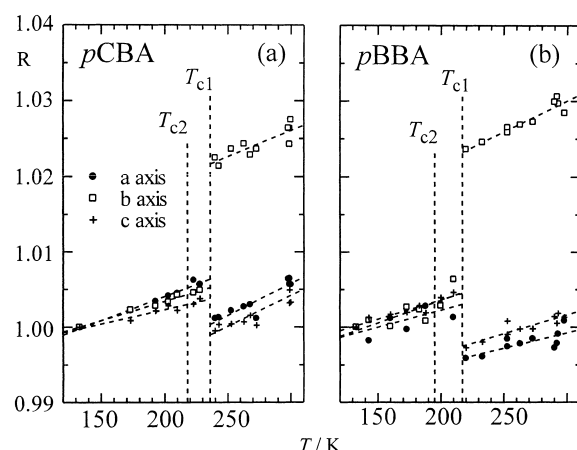
Fig. 1. Temperature dependence of the normalized lattice constants: $R = l(T)/l(133)$, where $l(T)$ denotes the length of the *a*, *b* or *c* axis at *T* K. The broken lines correspond to the least squares best fit on the assumption of a linear *T* dependence of *l*.

*p*CBA and *p*BBA were included in the refinement with anisotropic displacement parameters. All hydrogen atoms of *p*CBA were included in the refinement with isotropic displacement parameters. In the case of *p*BBA, the hydrogen atom of the OH group (H1)

was included in the refinement without constraint for the diffraction data at every temperature. Other hydrogen atoms of *p*BBA were treated without or with constraints, depending on the diffraction data.

Details of the present crystal structure analyses have been deposited in the Cambridge Crystal Data Center under the number CCDC 192469 and 192470 for *p*CBA at 240 and 133 K, respectively, and CCDC 192471 and 192472 for *p*BBA at 220 and 133 K, respectively.

3. Results and Discussion

3.1. Phase Transitions and Temperature Dependence of the Unit Cell Parameters

The three phases of *p*CBA and *p*BBA belong to the same crystal system and the same space group. The crystal data for the LTP and RTP of the two compounds are given in Table 1.

As can be seen in Fig. 1 (a) and (b), the first-order phase transition of *p*CBA and *p*BBA at T_{c1} manifests itself in the discontinuous change in the lattice constants. The changes clearly indicate the first-order nature of the phase transitions, although the unit cell vol-
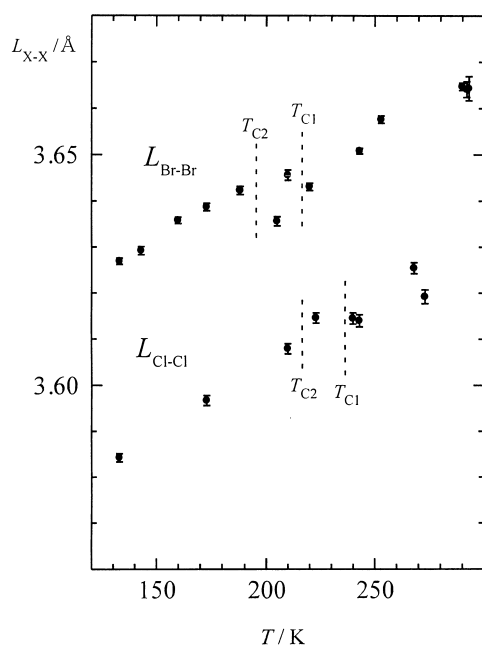
Fig. 2. Temperature dependence of the intermolecular halogen...halogen distance (L_{X-X}, X = Cl, Br) in A.

ume of both compounds showed only a subtle discontinuity of ca. 0.3% at T_{c1}. The occurrence of the phase transition of *p*CBA and *p*BBA at T_{c2} is ambiguous in the figure due to the higher-order of the transition. The intermolecular halogen...halogen distance (L_{X-X}) vs. *T* curves in Fig. 2, however, reveal the occurrence of the transition as a significant break at T_{c2}. The degree of the halogen···halogen overcrowding seems serious, especially in *p*BBA. These observations suggest that the close contact plays a certain role in the mechanism of the higher-order transition.

The thermal expansion coefficients of *p*CBA are $\Delta a/a = 6.4$, $\Delta b/b = 5.1$ and $\Delta c/c = 3.8$ [in *p*BBA, 4.5, 6.0 and 5.1]$\cdot 10^{-5}$K^{-1} for LTP and ITP, while 8.4, 6.0 and 8.3 [4.1, 8.0 and 5.0]$\cdot 10^{-5}$ K^{-1} for RTP. The magnitudes of the coefficients are comparable to those of *p*MBA [8] and usual organic crystals, for example benzoic acid [10] and α, ω-alkanedicarboxylic acids [11]. They do not show such a remarkable anisotropy as found for resorcinol, which has been attributed to the strong tendency of molecular realignment leading to the phase transition of that compound [12]. Approximately isotropic expansion of the present compounds seems to be consistent with the absence of a strong anisotropic molecular realignment related to the first-order transition (see, below).

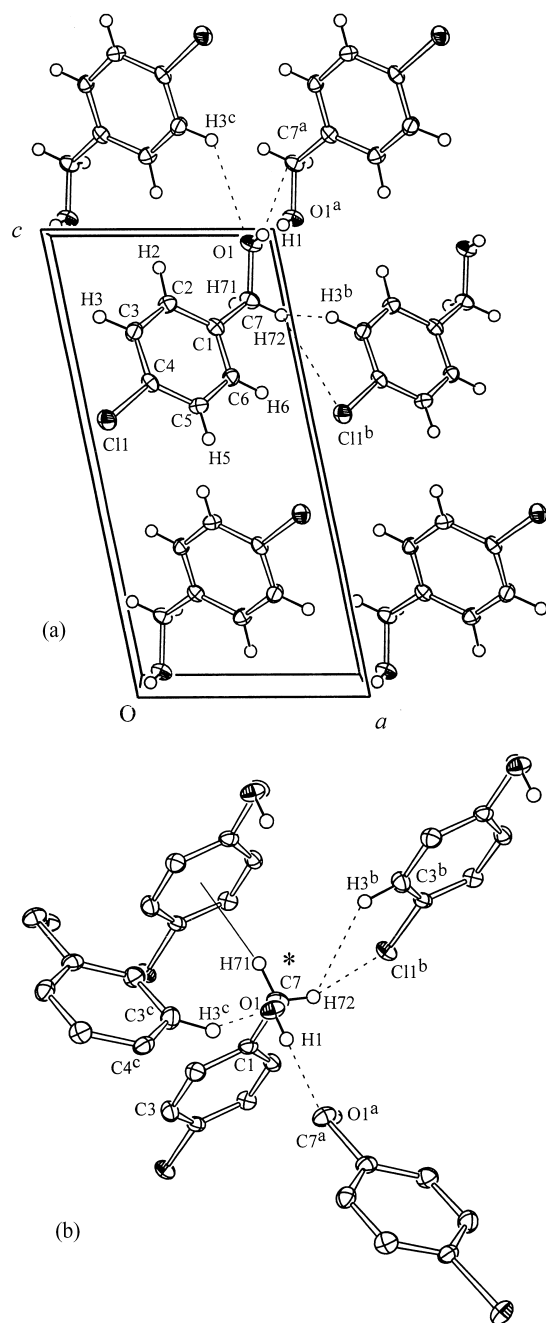## 3.2. Temperature Dependence of the Crystal and Molecular Structure

The three phases of the two compounds adopt almost the same structure, and the corresponding phases are isomorphic. The crystal structure of *p*CBA at 133 K is depicted in Fig. 3 (a), together with the atomic numbering. In Fig. 3 (b) are shown several intermolecular interactions including a C-H...π interaction mentioned later. The geometry of the C3[c]-H3[c]...O1 contact seems to indicate a weak C-H...O H-bond.

In each of the three phases, the molecules are arranged to form the linear O-H...O H-bonded chain illustrated in Figure 4.

Although the crystal structures of the three phases are substantially identical, the molecular structure of the RTP differs clearly from those of the ITP and LTP, as evidenced by the discontinuous jump of the torsion angle O1-C7-C1-C2 (χ) at T_{c1} (see, Fig. 5). On the other hand, the orientations of the C2-C6 and C1-C4 vectors with respect to the three crystal axes were found to exhibit subtle changes (< ca. 2°) at T_{c1}. These facts indicate that the orientation of the benzene ring is almost temperature independent, leading to the conclusion that the jump of χ can be attributed mostly to a displacement of the oxygen atom.

The conformation around the C7-O1 bond also changes markedly at T_{c1}: the torsion angles C1-C7-O1-H1 (ψ) of *p*CBA are 60(3)° (ITP, 223 K) and 166(4)° (RTP, 240 K). As a result, the position of the hydroxyl hydrogen atom (H1) with respect to the benzene ring shifts from the *cis*- to the *trans*-position at T_{c1}, as can be seen in Fig. 3 (b). A similar conformational change was observed for *p*BBA, the magnitudes of ψ being 68(9)° (ITP, 210 K) and 179(7) ° (RTP, 243 K).

In relation to the conformational change around C7-O1 one should point out the overcrowding between H1 and C7[a] in LTP and ITP (see Fig. 3 (b)). It seems to make the *cis*-position of H1 in LTP and ITP unstable on the increase in temperature, so that the H1 atom is expelled from the *cis*- to the *trans* position in the RTP as the transition from the ITP takes place. In the RTP of *p*CBA, the overcrowding between H1 and C7[a] atoms disappears. But, on the other hand, the contact between H72 and H3[b] and that between H72 and the chlorine atom (Cl1[b]) seem to become serious in the RTP (H72...H3[b]: 2.32(7) A; H72...Cl1[b]: 2.99(5) A at 240 K). The instability of the orientation of the OH

(a)

(b)

←— Fig. 3. (a): the crystal structure of the LTP of the *p*CBA at 133 K, viewed along the *b* axis. (b): the arrangement of the molecules viewed approximately along the O1-C7 bond. The broken lines indicate several short intermolecular contacts in *p*CBA. Their lengths (in A) are: H1...C7^a = 2.69(4) [2.79(9)] (the value in brackets for *p*BBA at 133 K); O1...C7^a = 3.344(4) [3.313(8)]; H72...H3^b = 2.47(6) [2.66]; H72...halogen^b = 3.09(4) [3.18]; O1...H3^c = 2.78(3) [2.74]; O1...C3^c = 3.469(3) [3.462(7)]. The symmetry codes: a: $2 - x$, $-0.5 + y$, $2 - z$; b: $1 + x$, $1 + y$, z; c: $1 - x$, $0.5 + y$, $2 - z$. The asterisk and a light solid line given in (b) denote the approximate position of H1 in the RTP and the C-H...π interaction, respectively.
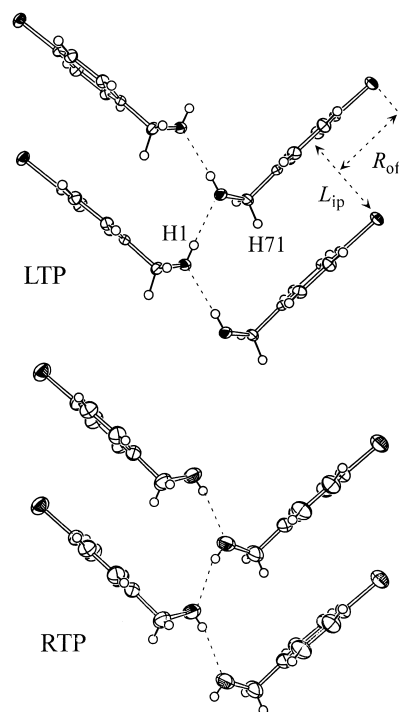

Fig. 4. Alignment of the *p*CBA molecules in the O-H...O H-bonded chain formed along the two-fold screw axis. The intermolecular O...O distance in A: 2.752(2) (133 K) and 2.741(3) (240 K) [for *p*BBA: 2.771(5) (133 K) and 2.747(4) (243 K)]. The notations L_{ip} and R_{off} are the interplanar distance between the aromatic rings and the ring offset, respectively.

group around the C1-C7 bond due to these close contacts in the RTP seems to be responsible for the significantly large U_{eqv} value characteristic of the O1 atom (0.0559(8) A^2 at 240 K) when compared to the average value of the carbon atoms (ca. 0.037 A^2), suggesting a reorientational vibration around the C1-C7 bond with fairly large amplitude.

Similar intermolecular interactions existing in *p*BBA are slightly different from those in *p*CBA, but the intermolecular contacts change significantly between the two compounds as demonstrated by, for examples, the halogen...halogen and O1···C7^a contacts. In fact, the ^{2}H NMR studies revealed remarkable differences in the lattice dynamics between the two compounds [8].
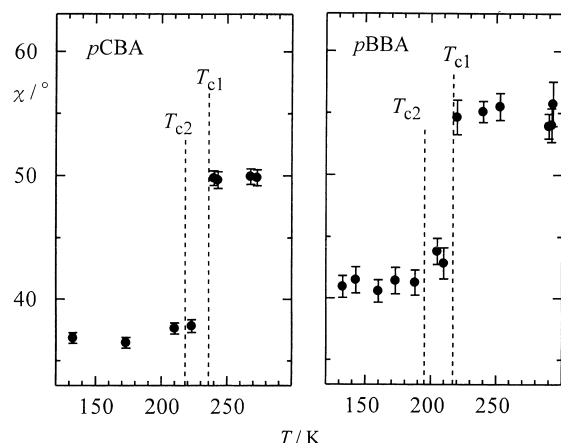
Fig. 5. Temperature dependence of the torsion angle C2-C1-C7-O1 (χ) of *p*CBA and *p*BBA.

The two kinds of conformational changes mentioned earlier seem to be coupled to cause the reversal of the direction of the hydrogen bond. As to the mechanism of the reversal of the hydrogen bond, there are, in general, two possibilities, that is conformational and configurational ones [13]. The former seems favorable in the present case, judging from the O...O distance in the H-bonded chain.

The O...O distance did show a slight discontinuity at T_{c1}: it decreases in the RTP by ca. 0.03 and 0.02 A for *p*CBA and *p*BBA, respectively, indicating a slight change in the nature of the O-H...O H-bond.

The C7-O1 bond length (L_{C-O} of *p*CBA decreases discontinuously at T_{c1} (L_{C-O}/A = 1.430(3) at 133 K and 1.388(4) at 240 K), whereas the C7-C1 bond length (L_{C-C}) is temperature independent (L_{C-C}/A = 1.502(4) at 133 K and 1.504(5) at 240 K). In the case of *p*BBA,

and L_{C-O}/A = 1.427(9) at 133 K and 1.369(7) at 243 K, and L_{C-C}/A = 1.499(9) at 133 K and 1.503(7) at 243 K. The L_{C-O} in RTP is significantly shorter than the standard length of the C(sp^3)-O bond in the C_{ar}-CH$_2$-OH fragment (1.426 A) [14], while L_{C-C} agrees with the standard of the C(sp^3)-C_{ar} bond (1.510 A). The change in the nature of the H-bond at T_{c1} would be responsible for the contraction of the L_{C-O}.

3.3. C-H...π Interaction

For organic monomers containing the X-benzyl group ($C_6H_5CH_2X$- where X = C, N, O), the CH...phenyl interactions have been classified into two types [15]. The first type is found in the column structure similar to that illustrated in Fig. 4 and characterized by the interplanar distance between the aromatic rings (L_{ip}) and the ring offset (R_{off}) in the column: L_{ip} = 3.4 - 3.7 A and R_{off} = 2.9 - 3.8 A [15]. The values of L_{ip} and R_{off} found for *p*CBA are on average 3.61 and 3.13 A in LTP [in LTP of *p*BBA, 3.65 and 3.15 A, respectively], suggesting the presence of the C-H...π interaction shown in Figure 3 (b). L_{ip} is constant within the estimated standard deviation regardless of the temperature, while the value of R_{off} shows a discontinuous decrease of ca. 0.15 A at T_{c1}. The latter observation indicates a slight variation of the character of the C-H...π interaction at T_{c1}.

[1] A. Katrusiak, Acta Crystallogr. **B56**, 872 (2000).
[2] S. R. Byrn, D. Y. Curtin, and I. C. Paul, J. Amer. Chem. Soc. **94**, 890 (1972).
[3] M. Hashimoto, M. Harada, M. Mizuno, M. Hamada, T. Ida, and M. Suhara, Z. Naturforsch. **57a**, 388 (2002).
[4] H. Niki, K. Kano, and M. Hashimoto, Z. Naturforsch. **51a**, 731 (1996).
[5] M. Hashimoto, Y. Monobe, H. Terao, H. Niki, and M. Mano, Z. Naturforsch. **53 a**, 436 (1998).
[6] M. Hashimoto, Y. Nakamura, and K. Hamada, Acta Cryst. **C44**, 482 (1988).
[7] M. Hashimoto and H. Fuess, unpublished data.
[8] M. Mizuno, M. Hamada, T. Ida, M. Suhara, and M. Hashimoto, Z. Naturforsch. **57a**, 381 (2002).

[9] G. M. Sherdrick, "SHELXL-97, Program for the Refinement of Crystal Structures", Univ. Goettingen, Germany 1997.
[10] C. C. Wilson, N. Shankland, and A. J. Florence, J. Chem. Soc., Faraday Trans. **192**, 5051 (1996).
[11] V. R. Thallaid, M. Nuesse, and R. Boese, J. Amer. Chem. Soc. **122**, 9227 (2000).
[12] G. E. Bacon and E. J. Lisher, Acta Cryst. **B36**, 1908 (1980).
[13] G. A. Jeffrey, "An Introduction to Hydrogen Bonding", Oxford University Press, Oxford 1997, Chapt. 7.
[14] F. H. Allen, O. Kennard, D. G. Watson, L. Brammer, A. G. Orpen, and R. Taylor, J. Chem. Soc., Perkin Trans. II, **1987**, S1.
[15] Z. Ciunik and S. Jarosz, J. Mol. Struct. **442**, 115 (1998).